ResearchGate

See discussions, stats, and author profiles for this publication at: https://www.researchgate.net/publication/257666174

Theoretical studies on the reaction mechanism and kinetics of the atmospheric reactions of 1,4-thioxane with OH radical

ARTICLE *in* STRUCTURAL CHEMISTRY · OCTOBER 2012

Impact Factor: 1.84 · DOI: 10.1007/s11224-012-9955-8

CITATIONS
16

READS
30

3 AUTHORS, INCLUDING:

L. Sandhiya
Ludwig-Maximilians-University of Munich
13 PUBLICATIONS **35** CITATIONS
SEE PROFILE

K. Senthilkumar
Bharathiar University
77 PUBLICATIONS **1,442** CITATIONS
SEE PROFILE

Available from: L. Sandhiya
Retrieved on: 23 January 2016

Struct Chem (2012) 23:1475–1488
DOI 10.1007/s11224-012-9955-8

ORIGINAL RESEARCH

Theoretical studies on the reaction mechanism and kinetics of the atmospheric reactions of 1,4-thioxane with OH radical

L. Sandhiya · P. Kolandaivel · K. Senthilkumar

Received: 12 December 2011 / Accepted: 23 January 2012 / Published online: 5 February 2012
© Springer Science+Business Media, LLC 2012

Abstract The volatile organic compounds (VOC) are emitted as pollutants into the atmosphere from many natural and artificial sources. The oxidation of VOC by the atmospheric species plays a key role in the degradation of VOC. In this investigation, the atmospheric degradation of a cyclic organosulfur compound 1,4-thioxane by OH radical is studied. The pathways for the reaction of 1,4-thioxane with OH radical have been modeled through electronic structure calculations using density functional theory at B3LYP and M06-2X level of theories with 6-31G(d,p) basis set. The structures, energies, and vibrational frequencies obtained from DFT calculations were subsequently used to perform canonical variational transition-state theory calculations to determine the rate constants over the temperature range of 278–350 K and to study the lifetime of 1,4-thioxane in the atmosphere. The OH-initiated reaction of 1,4-thioxane was found to proceed by hydrogen atom abstraction reaction and subsequent O_2 addition, leading to the formation of peroxy radical intermediate, which further undergoes secondary reactions with other atmospheric species. The possibility for the formation of various products from the oxidation of 1,4-thioxane in the atmosphere and their environmental implications are discussed. The rate constant calculated for the reaction of 1,4-thioxane with OH radical is in good agreement with the available experimental data.

Keywords 1,4-thioxane · OH radical · Atmospheric reactions · Activation energy · Rate constant

L. Sandhiya · P. Kolandaivel · K. Senthilkumar (✉)
Department of Physics, Bharathiar University,
Coimbatore 641 046, India
e-mail: ksenthil@buc.edu.in

Introduction

Volatile organic compounds (VOC) are emitted as pollutants into the atmosphere from anthropogenic and biogenic sources [1–5]. These compounds can undergo a series of chemical reactions, leading to their removal from the troposphere or transformation into other compounds. The possible degradation process for these VOC is their reactions with OH and NO_3 radicals. These radicals are important atmospheric constituents that are involved in the oxidation and production of many atmospheric species. The reactions of VOC with these radicals can also lead to the formation of ozone which is the major constituent of photochemical smog [6]. Also, a substantial portion of the VOC is degraded by reaction with ozone [7]. These reactions can form products that can be harmless, less harm, or even hazardous to life on earth. Among the various atmospheric oxidants, OH radical reacts exclusively with VOC and plays an important role in determining the lifetime of VOC in the atmosphere [8, 9]. Hence, it is very important to study the reaction between VOC and OH radical to know about the different degradation pathways. Also, the kinetics of the reactions is essential to find the lifetime of VOC emitted into the atmosphere and to understand the environmental implications.

The reaction kinetics of sulfur-containing VOC was studied and reported in various articles [6, 10–13]. The cyclic organosulfur compound 1,4-thioxane is a breakdown product of a chemical weapon agent called mustard gas when it is disposed in the sea [14, 15]. These organosulfur compounds are released into the atmosphere as a result of fossil fuel refining and combustion [6]. Recently, the kinetics of the reaction of 1,4-thioxane with OH, NO_3, and O_3 was evaluated experimentally by Atkinson and co-workers [16]. They measured the rate constants for the

reaction of 1,4-thioxane with OH radical over the temperature range of 278–350 K and with NO_3 and O_3 at room temperature. The rate constants for OH radical reactions with 1,4-thioxane was found to decrease with increasing O_2 concentration. In the atmosphere, the OH radicals can react with 1,4-thioxane during daylight [1]. The room temperature rate constant for the reactions of OH, NO_3, and O_3 with 1,4-thioxane was reported as 2.0×10^{-11}, 5.9×10^{-14}, and $<2.5 \times 10^{-19}$ cm^3 $molecule^{-1}$ s^{-1}, respectively, and it has been found that the OH radical reactions with 1,4-thioxane proceeded by H atom abstraction from the CH_2 groups of 1,4-thioxane [16]. The reaction between 1,4-thioxane and OH radical involve in aerosol formation (oxidation of SO_2 by carbonyl oxides) [16] and hence the atmospheric effects of these reactions are potentially important.

Previous studies [17–19] on the reactions of VOC with OH radical have shown that the reactions involve two key intermediates, a peroxy radical and an alkoxy radical. As shown in Fig. 1, the alkyl radical formed through the abstraction of hydrogen atom from the CH_2 group of 1,4-thioxane further reacts with O_2 to form alkyl peroxy radical as the first key intermediate. This alkyl peroxy radical interact with NO and produce NO_2 and an alkoxy radical which is the second key intermediate. Again in the presence of NO_2, the alkoxy radical further react with O_2, yielding ozone. Thus, peroxy radical serve as a precursor of ozone formation in the troposphere. The alkyl peroxy radical can also react with HO_2 to produce an hydroperoxide of 1,4-thioxane. An important characteristic of alkyl peroxy radical is its capability to undergo a self-reaction [20, 21]. These self-reactions involve tetraoxide intermediate which again decomposes into new products. Thus, multiple reaction pathways for the reaction of 1,4-thioxane with OH radical are possible and have to be studied in detail.

To the best of our knowledge, the details of reaction mechanism of organosulfur compounds with OH are very limited. Except for the initial hydrogen atom abstraction step [16], the reaction mechanisms and kinetics of secondary reactions of 1,4-thioxane has not been studied. To understand the atmospheric implications, the complete knowledge of the reaction mechanism is very essential. Hence, the experimental studies of Atkinson et al. [16] should be combined with a theoretical study to analyze the different pathways for OH reactions with 1,4-thioxane. In view of the above-mentioned exposures, the principal aim of this study is to model the different reaction pathways and kinetics of the reactions of 1,4-thioxane with OH radical. The transition states corresponding to possible intermediates and products are located to identify and characterize the reaction pathways. The kinetics of the most favorable reactions is studied using variational transition state theory (VTST) [22]. Through theoretical results, the oxidation of 1,4-thioxane and its atmospheric implications are discussed.

Computational methods

The geometry of the minima and first-order saddle points on the potential energy surface of the reactions of 1,4-thioxane with OH radical were optimized using density functional theory methods B3LYP [23, 24] and M06-2X

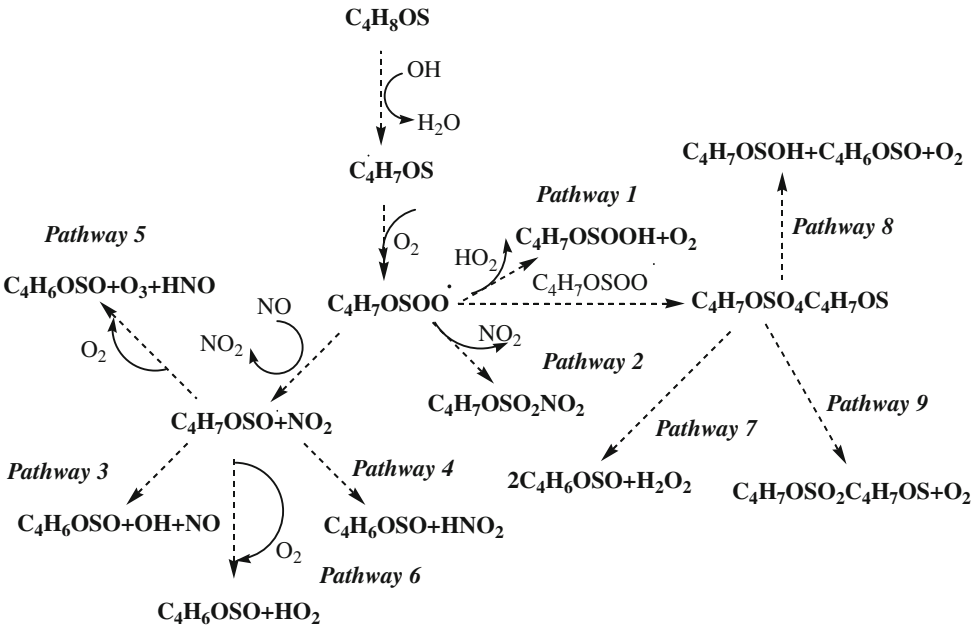

Fig. 1 Reaction scheme for the OH-initiated reactions of 1,4-thioxane

[25] with 6-31G(d,p) basis set. Previous studies on atmospheric reactions show that the structures and energies obtained with B3LYP method is comparable with the results of MP2, CCSD(T), and QCISD methods [7, 26, 27]. It has also been concluded that the DFT calculations with M06-2X functionals perform well for thermochemical and reaction mechanism studies [28, 29]. In the present investigation, the structure and energy of reactants, intermediates, transition states, and products are obtained using B3LYP and M06-2X functionals. The electronic structure calculations were also performed with 6-31+G(d,p) basis set for the most favorable reaction pathway. The harmonic vibrational frequencies were calculated for all the optimized geometries to verify the nature of the stationary points. All minima were confirmed with positive frequencies, while each transition state had one imaginary frequency confirming their location as maxima in one reaction coordinate. Note that the optimization and frequency calculations were performed at the above two level of theories. Curvilinear coordinate system was used to calculate the generalized normal frequencies. The connection of transition state structure between designated reactant and product has been confirmed in each case by intrinsic reaction coordinate (IRC) calculations at B3LYP/6-31G(d,p) level of theory using the second order algorithm of Gonzalez and Schlegel [30, 31]. The enthalpy of a reaction and barrier height were calculated by including thermodynamic correction to the potential energy surface. The thermodynamic calculations were carried out at 298.15 K and 1 atm of pressure. All the electronic structure calculations were performed using Gaussian09 program package [32].

The theoretical rate constants for the most favorable reactions of 1,4-thioxane with OH radical were calculated using canonical variational transition state theory (CVT) [33–35]. The quantum effect correction for the CVT rate constant has been made by small curvature tunneling (SCT) calculations [36, 37]. The potential energy surface, gradients, and hessians obtained from M06-2X/6-31G(d,p) electronic structure calculations were directly used to calculate the rate constants. Through CVT, the rate constant at temperature T is given by,

$$k^{\mathrm{CVT}}(T) = \min_{S} k^{\mathrm{GT}}(T, s), \tag{1}$$

where

$$k^{\mathrm{GT}}(T, s) = \frac{\sigma k_{\mathrm{B}} T}{h} \frac{Q^{\mathrm{GT}}(T, s)}{\varphi^{R}(T)} e^{-V_{\mathrm{MEP}}(s)/k_{\mathrm{B}}T}, \tag{2}$$

where $k^{\mathrm{GT}}(T, s)$ is the generalized transition state theory rate constant at the dividing surface s, σ is the symmetry factor accounting for the possibility of more than one symmetry related reaction path, k_{B} is Boltzmann's constant, h is Planck's constant, $\phi^{\mathrm{R}}(T)$ is the reactant partition function per unit volume, and $Q^{\mathrm{GT}}(T, s)$ is the partition function of a generalized transition state at s. The partition functions for most of the vibrational modes were evaluated by treating them as quantum mechanically separable harmonic oscillators, while the lowest vibrational mode was evaluated by hinder-rotor approximation [38, 39]. The rate constant calculations were performed by using GAUSSRATE 2009A [40] program which is an interface between Gaussian09 and POLYRATE 2010A [41] programs.

Results and discussion

Reaction mechanism and reaction paths

The proposed reaction scheme for the reactions of 1,4-thioxane with OH radical is illustrated in Fig. 1. The structures of stationary points in the ground state potential energy surface of the reaction system optimized at the M06-2X/6-31G(d,p) level of theory are shown in Figs. 2, 4, 6, and 8. The energy profile corresponding to different pathways of the reaction of 1,4-thioxane with OH radical obtained using M06-2X/6-31G(d,p) are illustrated in Figs. 3, 5, 7, and 9. The energy barrier (ΔE), enthalpy (ΔH), and Gibbs free energy (ΔG) of the reactive species calculated at B3LYP/6-31G(d,p) and M06-2X/6-31G(d,p) levels of theory are summarized in Table 1. The energetics obtained for the most favorable reaction pathway using B3LYP and M06-2X functionals with 6-31+G(d,p) basis set is given in Table 2. The selected geometrical parameters of the optimized structures of the most favorable reaction pathway calculated at B3LYP and M06-2X functionals with 6-31G(d,p) and 6-31+G(d,p) basis sets are summarized in Table 3. The structural parameters of the reactive species obtained from DFT calculations with the above two exchange correlation functionals differ slightly. For instance, the average root-mean-square deviation (rmsd) between the internal coordinates obtained from B3LYP and M06-2X methods with 6-31G(d,p) basis set is 0.06 Å for the reactants, 0.1 Å for the transition state, and 0.3 Å for the products for the favorable reaction path in the studied reaction mechanism. The average rmsd between the internal coordinates obtained using the two methods with 6-31+G(d,p) basis set for the most favorable reaction path is 0.05, 0.1, and 0.4 Å for the reactant, transition state, and product, respectively. The above-mentioned rmsd between the internal coordinates obtained with the two methods is due to a slight change in optimized bond angle and dihedral angle values (see Table 3). While comparing the results obtained from B3LYP and M06-2X methods, it is found that the B3LYP method underestimates the energy barrier

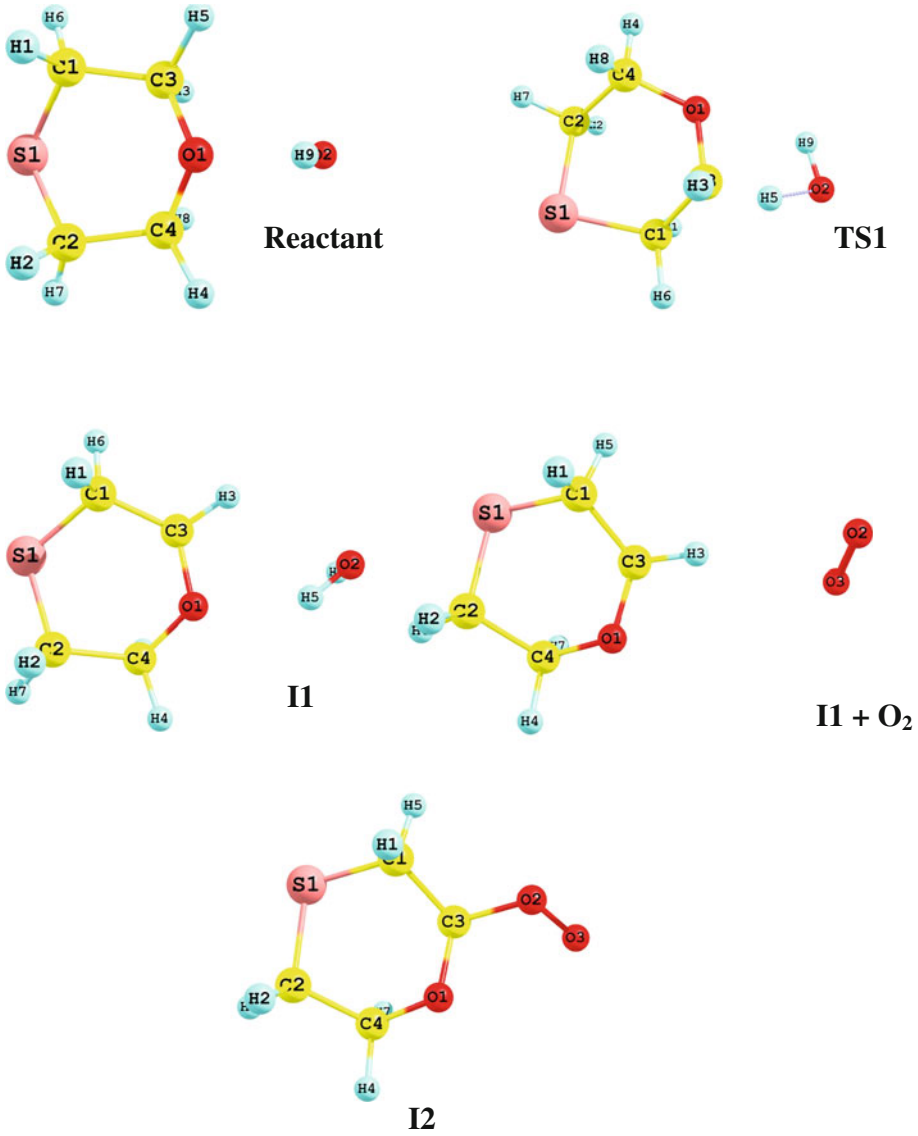

Fig. 2 The optimized structures of the reactive species corresponding to the formation of peroxy radical I2 from the OH-initiated reaction of 1,4-thioxane

by 6–13 kcal/mol. Also, from Table 2, it is observed that the use of diffuse function in the 6-31G(d,p) basis set at B3LYP level significantly alters the energetics of the reaction between 1,4-thioxane and OH radical, but the results obtained at M06-2X/6-31+G(d,p) level of theory is comparable to the results obtained at M06-2X/6-31G(d,p) level of theory. While quantitatively comparing the results obtained from the above two methods for various reaction pathways, it is observed that the relative importance of these reaction pathways does not change with respect to exchange correlation functionals used in DFT calculations, i.e., the favorable reaction path obtained using B3LYP functional is the same in M06-2X functional also. The structure and energetics obtained using M06-2X functional with 6-31G(d,p) basis set are discussed in detail and are used in further kinetic calculations. Note that an error of 2 kcal/mol in barrier height will lead to an error in calculated rate constant by one order of magnitude depending upon the temperature [42]. The intermediates, transition states and products are labeled as I, TS and P, respectively, followed by a number.

The active reactive site of 1,4-thioxane is the carbon atom nearer to the oxygen atom for reaction with OH radical [16]. This reaction is initiated by the abstraction of H atom from the CH_2 group of 1,4-thioxane by OH radical producing 1,4-thiooxonium radical (I1) and a water molecule. This abstraction reaction is analogous to the reactions of OH with VOC having alkyl groups [43–45]. The

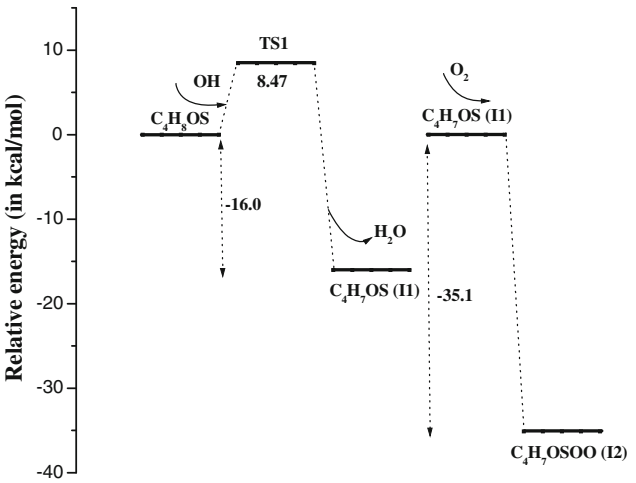

Fig. 3 Relative energy profile corresponding to the formation of peroxy radical from OH-initiated reaction of 1,4-thioxane

abstraction of H atom is caused by the transition of an electron in σ orbital of the C–H covalent bond to the nonbonding orbital in the OH radical. As reported in Table 1, the hydrogen atom is abstracted via an apparent barrier of 8.47 kcal/mol at the transition state (TS1). As given in Table 3, in the transition state structure (TS1), the bond distance between the abstracted H atom (H5) and O atom of OH decreases by 1.8 Å from that of the reactant. The HOH (H5–O2–H9) bond angle is about 104° in the product which was 47.6° in the initial reactants. This reaction was found to be exothermic and exergonic with $\Delta H = -16$ kcal/mol and $\Delta G = -17.42$ kcal/mol at 298.15 K, respectively. It is obvious from the earlier studies that H atom abstraction reactions are exothermic [45–47]. As depicted in Fig. 1, the radical I1 formed in the abstraction channel is found to undergo a secondary reaction with oxygen molecule. The oxygen molecule binds with the carbon atom at which the hydrogen atom was abstracted and a key intermediate, hydroxyl-1,4-thioxane peroxy radical (I2) is formed. The oxygen addition reaction proceeds without any barrier and this intermediate formation is exothermic by −29.95 kcal/mol and is exergonic by −32.02 kcal/mol. The bonding between C_3H_7OSC (I1) and OO fragments is relatively weak and hence the reaction leading to peroxy radical formation is reversible under tropospheric conditions and this result in chemical equilibrium between I1 + O_2 and I2. In the atmosphere, the hydroxyl-1,4-thioxane peroxy radical can further undergo reactions with other radicals and with itself leading to multiple reaction pathways. The mechanism of the reaction pathways to several dissociation products are discussed below.

As shown in Fig. 1, the hydroxyl-1,4-thioxane peroxy radical intermediate (I2) reacts with HO_2 in the atmosphere leading to the formation of a stable product. The terminal O atom of peroxy radical has high electron affinity toward the hydrogen atom of HO_2. So, I2 will readily abstract the H atom of HO_2 and 2-hydroperoxy-1,4-thioxane (P1) is formed along with an oxygen molecule. The similar hydrogen abstraction reaction has been noted for the reaction between benzyl peroxy radical with HO_2 [48]. A transition state (TS2) with a very small barrier of 3.53 kcal/mol was identified for this product channel. The high electron affinity of I2 controls the barrier height and increases its reactivity toward HO_2. In the transition state structure (TS2), as given in Table 3, the bond length between H of HO_2 and O of peroxy radical has reduced from the reactants by 0.6 Å. This product is formed exothermically with the heat of reaction of −29.95 kcal/mol. The reaction is exergonic with a free energy of −32.02 kcal/mol. Several attempts were made to study the addition of HO_2 to peroxy radical I2. But all the attempts resulted in the formation of 2-hydroperoxy-1,4-thioxane (P1) along with O_2. A previous study reported that the oxygen molecule thus eliminated from RO_2 + HO_2 reactions was confirmed to be in its singlet state [49]. If the addition reaction takes place, the product will be a radical, which may further decompose to hydroperoxide and O_2. Hence, the direct abstraction of H atom from HO_2 by peroxy radical is most favored than addition reactions.

The second pathway studied is the reaction of the hydroxyl-1,4-thioxane peroxy radical (I2) with NO_2 in the atmosphere. This reaction is an important process during the oxidation of 1,4-thioxane, because traces of nitrogen oxides are often present in the atmosphere and may then be consumed in several atmospheric processes. This reaction was found to terminate radical chain reactions and produces alkyl nitrates, acting as NO_x reservoir compounds. In this reaction, the nitrogen atom of NO_2 is directly bonded with the oxygen atom of peroxy radical to form 1,4-thioxane-2-yl nitroperoxoate (P2). The reaction is characterized by a transition state (TS3) with a very large barrier of 119.02 kcal/mol. The transition state (TS3) involves the bonding of N of NO_2 with terminal O of peroxy radical with a bond length value less than that of the reactant by 0.6 Å. The reaction between I2 and NO_2 at the oxygen site is a barrier-consumed process due to the strong repulsion from the lone-pair electrons of O in NO_2. Also, the single unpaired electron is mainly positioned at the internal N-site of NO_2. So, I2 can attack NO_2 less favorably. As reported in Table 1, among all the reaction pathways studied, this pathway is highly endothermic and endergonic with ΔH of 52.2 kcal/mol and ΔG of 52.88 kcal/mol. This reaction is kinetically inaccessible due to the large barrier height. Also, the high endothermicity of the reaction shows that this reaction is unlikely to be of any significance under atmospheric conditions.

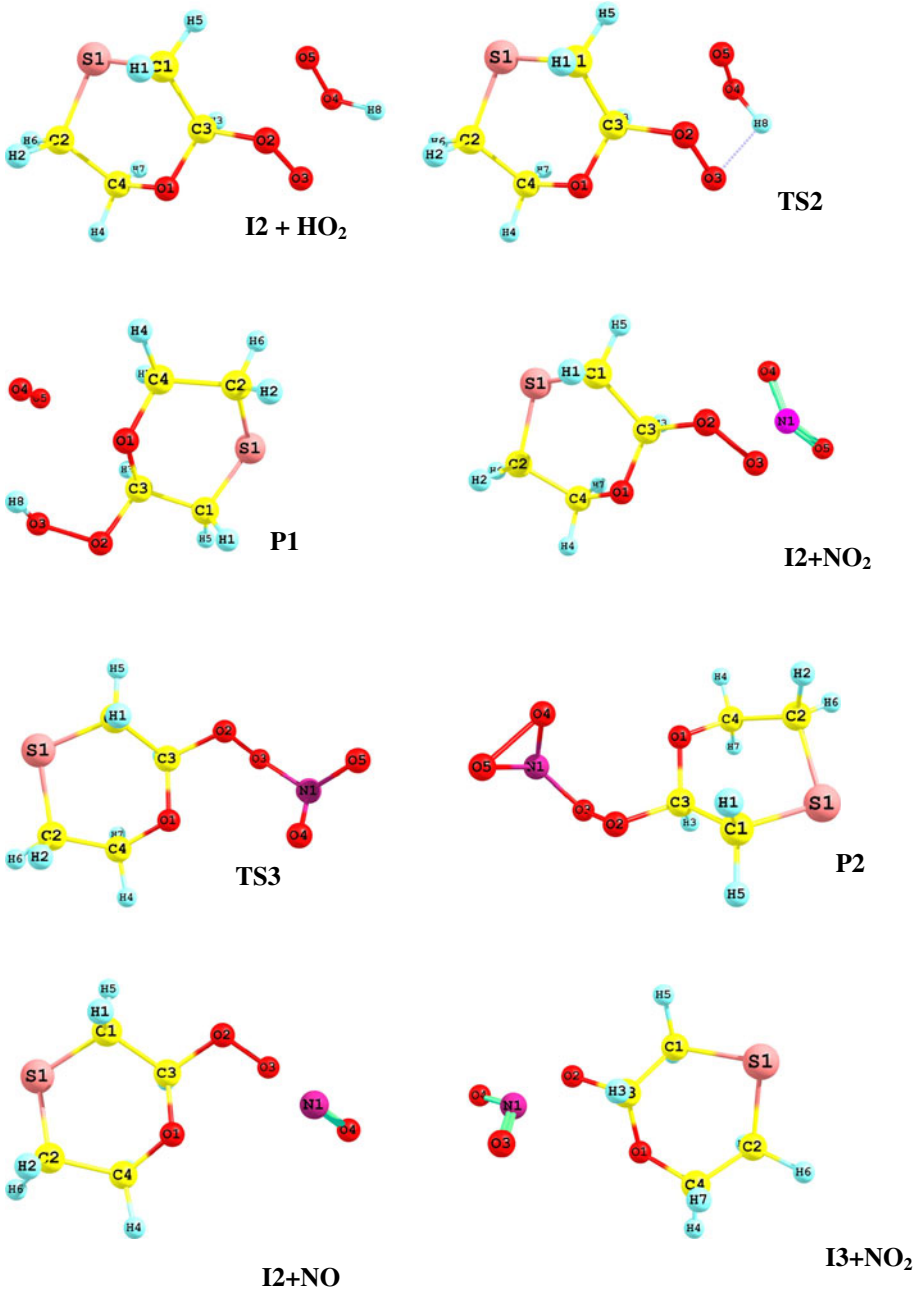

Fig. 4 The optimized structures of the reactive species corresponding to the reactions of peroxy radical I2 with HO_2, NO_2, and NO

The next significant pathway involved is the reaction of hydroxyl-1,4-thioxane peroxy radical (I2) with NO. During this attack, the O–O bond of the peroxy radical gets cleaved and NO is oxidized (see Fig. 4). Therefore, an alkoxy radical (I3) is formed and this is the second key intermediate in the reaction mechanism. This oxidation reaction occurs without any barrier. The intermediate I3 is formed exothermically with a reaction enthalpy of −30.0 kcal/mol and is exergonic by −29.37 kcal/mol. As this intermediate I3 is formed by prompt decomposition of exothermic I2 + NO reaction, this is an important intermediate in determining the products formed from 1,4-thioxane oxidation. As shown in Fig. 1, there are two branching processes possible for the reaction between I3 and NO_2. In one of the reactions, the intermediate (I3) can further undergo decomposition and regenerate OH and NO radicals along with 1,4-thioxane-2-one (P3). Here, the bond O–N of NO_2 is cleaved and the O atom readily abstracts the hydrogen atom from the C–H bond of alkoxy radical, thus forming OH radical. Hence, as shown in Fig. 6, a double bond is formed between atoms C and O of alkoxy radical (I3) to produce a neutral coproduct 1,4-thioxane-2-one.

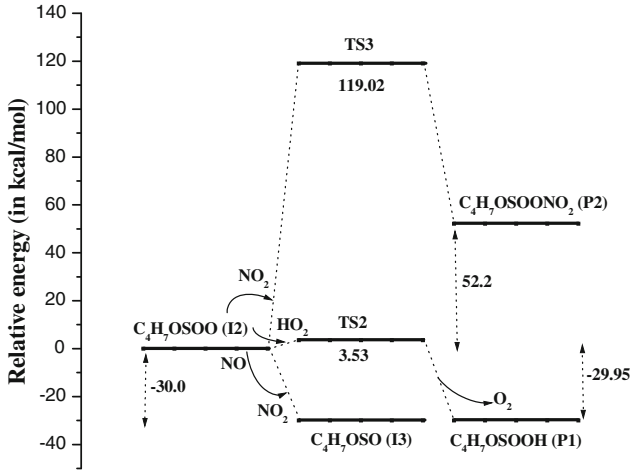

Fig. 5 Relative energy profile corresponding to the reactions of peroxy radical with HO_2, NO_2, and NO

The nonbonding-electron of CO group of I3 interacts with σ electron of NO_2 and thus an electron-rich π bond is formed between C and O atoms of I3 making the product more stable. This reaction is endothermic and endergonic by 22.57 and 19.76 kcal/mol, respectively. The formation of this product channel was associated with a transition state (TS4) of barrier height 29.06 kcal/mol. This reaction may be a significant atmospheric pathway due to the regeneration of OH and NO radicals.

In the other way, the alkoxy radical intermediate (I3) can also decompose by the direct abstraction of H atom in CH group by NO_2, which results in the formation of nitrous acid and the coproduct 1,4-thioxane-2-one (P4). This product channel is characterized by a transition state (TS5) with a barrier of 66.2 kcal/mol. As illustrated in Fig. 6, in the transition state (TS5), the H atom of alkoxy radical tries to bind with N atom of NO_2 and a hydrogen bonding of about 2 Å is noted. As given in Table 1, the formation of this product is exothermic with $\Delta H = -28.61$ kcal/mol and exergonic by -31.7 kcal/mol. Comparing the energy barriers in these two processes, it is asserted that the formation of P3 is kinetically favorable, because the barrier height for P4 formation is higher by 37 kcal/mol than that of P3. But, the enthalpy values in the two reactions show that the formation of P4 is the lowest energy pathway and hence this reaction is thermodynamically favored.

Another important pathway from I3 involves the formation of O_3 due to the reaction between alkoxy radical intermediate (I3) with NO_2 and O_2. This reaction is a prototype in which O_3 is formed due to OH-initiated reaction of VOC [50]. Here, one O atom from NO_2 binds with O_2 to form O_3 and the remaining NO abstracts the H atom from the alkoxy radical. The C–O group of alkoxy radical possesses double bond character. Thus 1,4-thioxane-2-one, O_3 and HNO (P5) are formed as products. The formation of this product channel is associated with a transition state (TS6) with a barrier of 79.02 kcal/mol. As shown in Fig. 6, in the transition state structure (TS6), the bond N–O of NO_2 is cleaved and O atom bind with O_2 to form a biradical of O_3 and the distance between O–O of this biradical is 0.8 Å greater with respect to the product. This reaction is endothermic and endergonic with ΔH of 23.61 kcal/mol and ΔG of 20.14 kcal/mol.

The majority of alkoxy radicals can potentially undergo reaction with O_2 [1]. In the reaction between alkoxy radical (I3) and O_2, the oxygen molecule is aligned in plane with the C–C bond in the transition state (TS7) and directly abstracts H atom from the C–H bonds of the alkoxy radical to form HO_2 and 1,4-thioxane-2-one (P6). The electron withdrawing O atom in O_2 directly abstracts H atom from C–H bond of I3 and hence the C–H bond acquires double bond character and become neutral (see Fig. 7). The reaction is highly exothermic and exergonic with a reaction enthalpy of -46.14 kcal/mol and free energy of -44.76 kcal/mol, respectively. The formation of the transition state (TS7) for this product is associated with a barrier of 9.9 kcal/mol. This reaction is kinetically accessible due to the small activation energy barrier. While comparing the reactions of alkoxy radical I3 with NO_2 and O_2, it is observed that, the reaction of I3 with O_2 is of potential importance in determining the fate of alkoxy radical resulting from 1,4-thioxane oxidation in the atmosphere.

The next most significant pathways are due to the self-reactions of the hydroxyl-1,4-thioxane peroxy radicals as illustrated in Fig. 1. The self-reactions of the peroxy radicals are characterized by the formation of a tetraoxide intermediate and the geometry of this intermediate determines the pathway [21]. In this case, the self-reactions involved a linear tetraoxide intermediate (I4) formation leading to three dissociation pathways. The intermediate (I4) is formed by the bonding of oxygen atoms on the self-reactants without any barrier. The formation of the intermediate (I4) is exothermic by -37.62 kcal/mol and exergonic by -39.11 kcal/mol. The peroxy radicals are responsible for the formation of hydrogen peroxides in the troposphere [20, 21]. As shown in Fig. 1, the tetraoxide intermediate (I4) decomposes into hydrogen peroxide. This process takes place due to the cleavage of C–H and the O–O bonds of the tetraoxide intermediate. Then, the cleaved hydrogen and oxygen atoms combine to form hydrogen peroxide and the coproduct is a carbonyl compound 1,4-thioxane-2-one (P7) (see Fig. 8). The formation of these compounds is characterized by a transition state (TS8) with a barrier height of 4.64 kcal/mol. As illustrated in Fig. 9, this reaction path is a highly exothermic with enthalpy of formation of -124.34 kcal/mol and is exergonic by -127.02 kcal/mol. Thus, this reaction is both kinetically and thermodynamically favored.

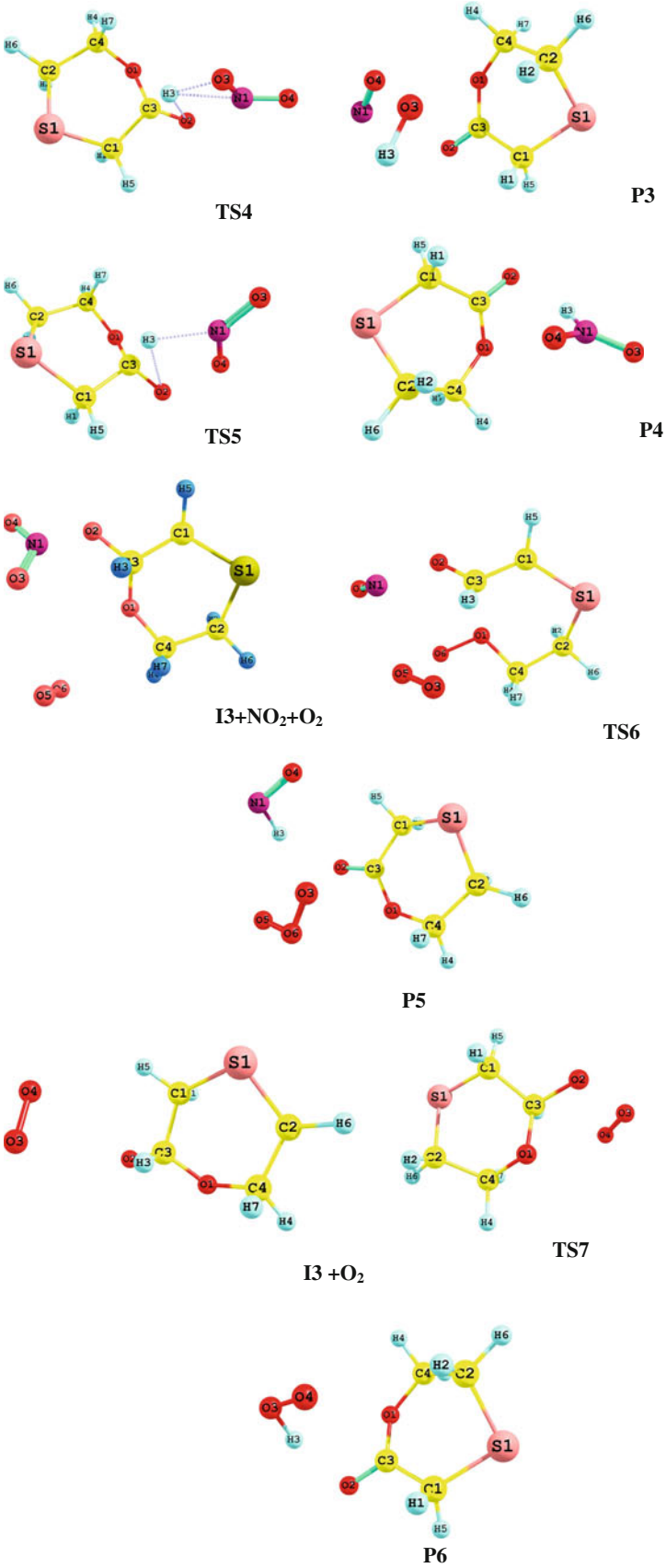

Fig. 6 The optimized structures of the reactive species corresponding to the reactions of alkoxy radical I3 with NO_2 and O_2

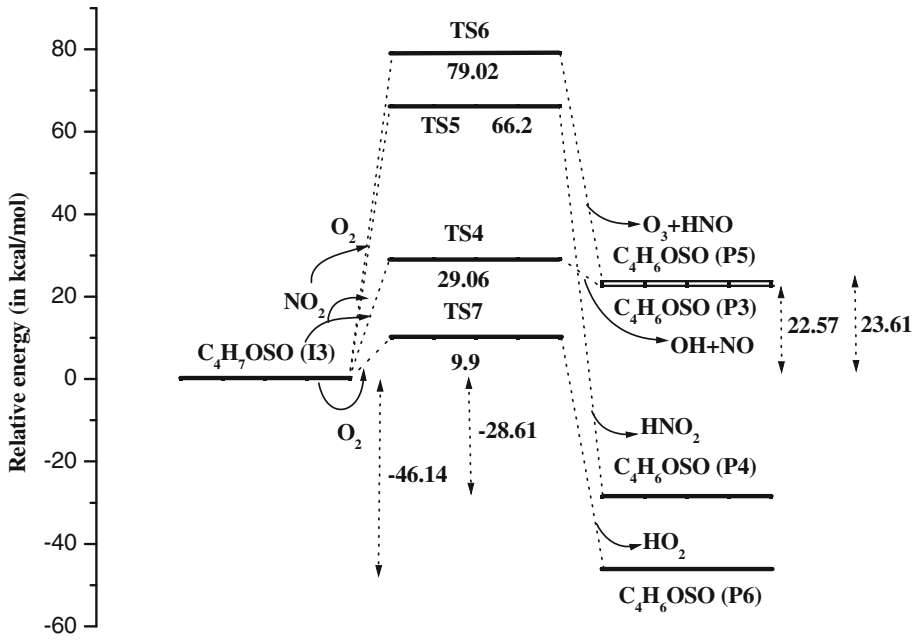

Fig. 7 Relative energy profile corresponding to the reactions of alkoxy radical with NO_2 and O_2

The intermediate (I4) further decomposes by the cleavage of O–O bonds of peroxy radical on both the reactants. This leads to the formation of an oxygen molecule, and the hydrogen from one of the peroxy radicals binds with the oxygen atom of other peroxy radical. This forms an alcoholic compound, 1,4-thioxane-2-ol and a carbonyl compound, 1,4-thioxane-2-one (P8). This product channel is formed via a transition state (TS9) with a barrier of 33.24 kcal/mol. As shown in Fig. 8, during the transition from intermediate (I4) to products (P8), one oxygen molecule is formed and there is a weak bonding between the oxygen atom of carbonyl compound and the hydrogen atom which is yet to attach with the neighboring radical to form the alcoholic compound. At this state, the hydrogen atom tries to bind with the oxygen atom of the oxygen molecule. This weak interaction makes the reacting species unstable and thus leads to the formation of product P8. This pathway is exothermic by −64 kcal/mol and is exergonic by −67.55 kcal/mol. This reaction is not so feasible due to the high pronounced barrier of TS9.

The self-reaction also proceeds by the formation of O_2 and the self-reactants are binded through the oxygen atoms to form a 2,2′-peroxy-bis-1,4-thioxane (P9). This product is formed through a transition state (TS10) with a barrier height of 35.6 kcal/mol. The transition state (TS10) forms two alkoxy radicals initially and the C–C bond length of alkoxy radical increased from 1.5 to 1.9 Å. Also, the distance between the oxygen atoms of the alkoxy radicals decreased by 1.1 Å than that of the tetraoxide intermediate (I4). The product channel is endothermic and endergonic by 6.12 and 3.6 kcal/mol, respectively. This reaction is of less significance in the atmosphere due to the pronounced barrier height. Among the studied self-reactions, the formation of product channel P7 is most favorable with a small barrier height of 4.64 kcal/mol and large exothermicity of −124.34 kcal/mol.

Kinetics

The reaction mechanisms and reaction pathways discussed in the above section show that the peroxy radical (I2) is the major intermediate in determining the oxidation of 1,4-thioxane in the atmosphere. From Table 1, it is observed that the formation of 2-hydroperoxy-1,4-thioxane along with O_2 is the most favorable reaction pathway resulting from OH-initiated reaction of 1,4-thioxane and subsequent O_2 addition to initial step. Hence, the rate constants are calculated only for the initial H atom abstraction (I1) step, the peroxy radical formation (I2) step, and the formation of hydroperoxide along with O_2 (P1) product channel. The rate constants are calculated using CVT with SCT corrections in a temperature range from 278 to 350 K with ZPE corrected energies, gradients and hessians calculated at M06-2X/6-31G(d,p) level of theory. The rate constants for hydrogen abstraction channel (I1), formation of peroxy radical intermediate channel (I2), and the product channel (P1) are designated as k_{I1}, k_{I2}, and k_{P1}, respectively, and the calculated rate constant values in the temperature range of 278–350 K are summarized in Table 3. The Arrhenius plots for the three reaction channels are shown in Fig. 10.

As it is evident from Table 4, the rate constants for hydrogen abstraction channel k_{I1} show a negative temperature dependence as observed for other VOC [6, 51]. The calculated rate constant k_{I1} for hydrogen abstraction

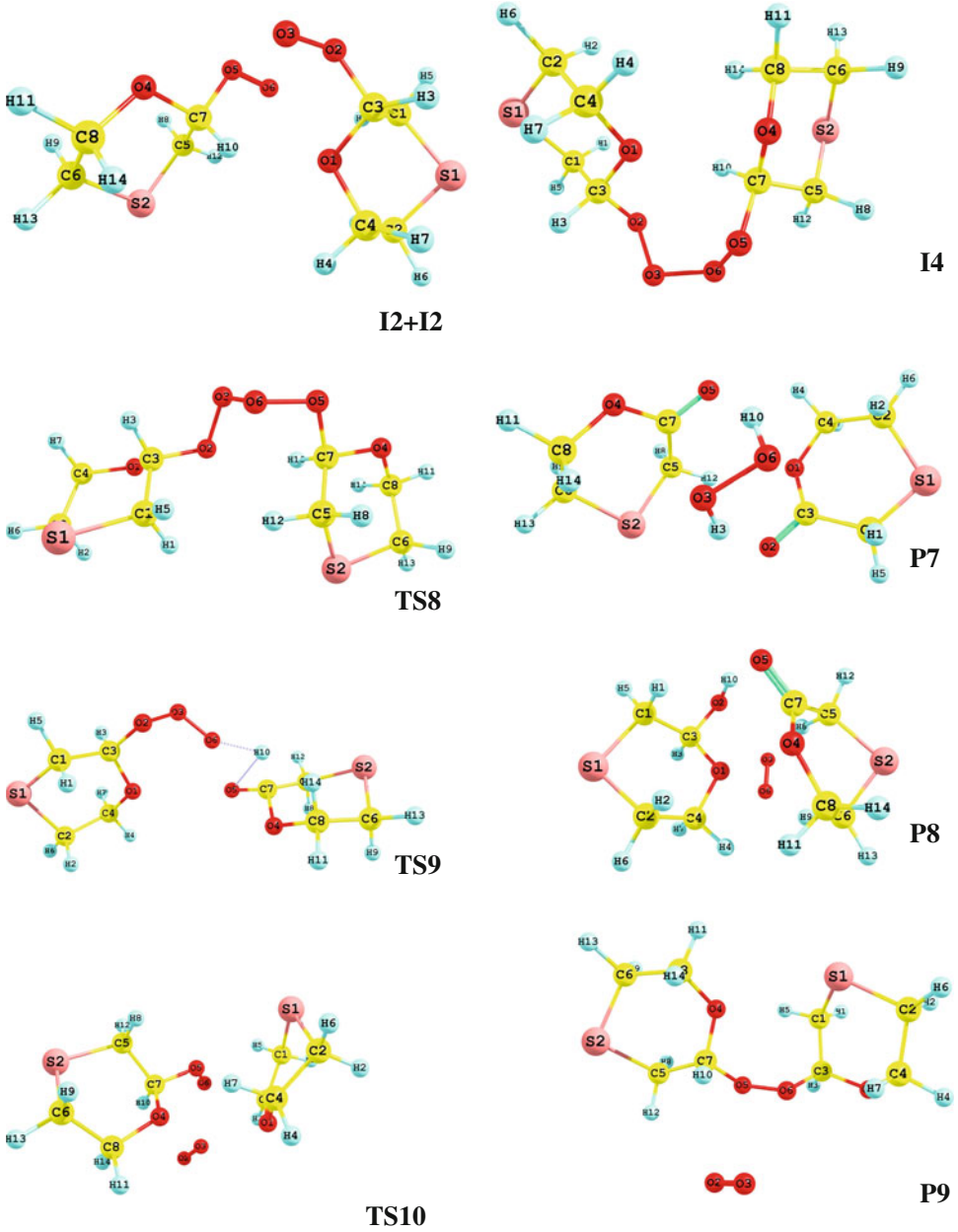

Fig. 8 The optimized structures of the reactive species corresponding to the self-reactions of peroxy radical I2

channel at 298 K is 5.8×10^{-16} cm^3 molecule^{-1} s^{-1}. This value is comparable with the IUPAC evaluated rate constant value of 1.14×10^{-17} cm^3 molecule^{-1} s^{-1} for the initial H atom abstraction reaction from alkyl group of dimethyl ether [52]. This calculated rate constant is attributed to the structure of 1,4-thioxane. The CH_2 group of 1,4-thioxane have electron donating character and can help to cope with the charge deficient OH radical which is having electron withdrawing character. Hence, the OH radical activates the H atom abstraction from CH_2 group of 1,4-thioxane and the reaction occurs dominantly. The tunneling factor for the initial abstraction step is negligible due to the broad energy barrier as suggested by the small imaginary vibrational frequency (-283.53 cm^{-1}) of TS1. The variation of k_{I1} with temperature is very small which suggests that the activation energies around 298 K should be close to zero. The Arrhenius activation energy calculated for this initial step at 298 K is 4.6 kcal/mol.

The peroxy radical intermediate (I2) is formed without potential barrier under the formation of a loose transition state. Hence, the rate constant for this channel is obtained by variationally moving the reference position along the minimum energy path. The forward rate constant calculated for the peroxy radical formation I2 at 298 K is

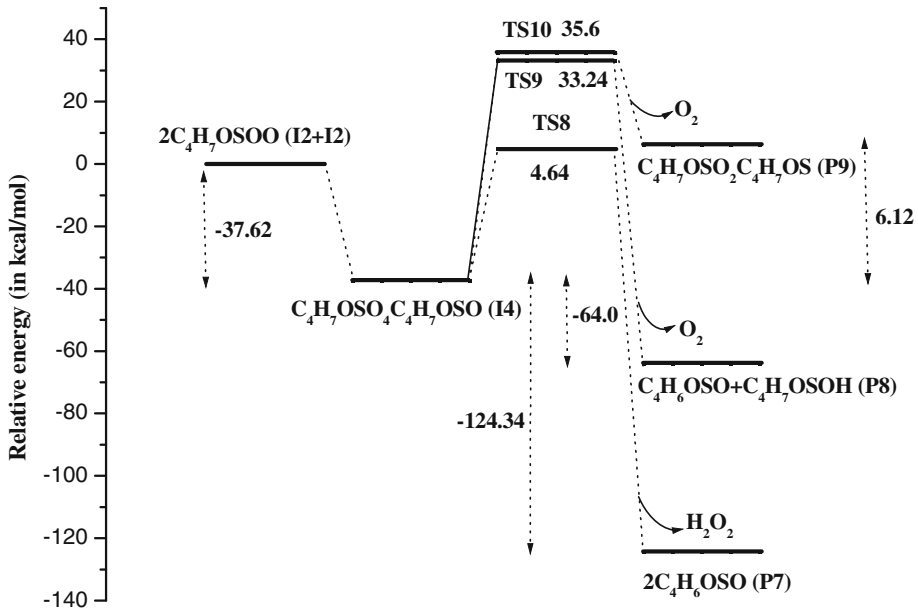

Fig. 9 Relative energy profile corresponding to the self-reactions of peroxy radical I2

Table 1 Energy barrier ΔE (in kcal/mol), enthalpy ΔH (in kcal/mol), and Gibb's free energy ΔG (in kcal/mol) for the proposed reactions of 1,4-thioxane with OH radical calculated at B3LYP/6-31G(d,p) and M06-2X levels of theory

Reactions	B3LYP/6-31G(d,p)			M06-2X/6-31G(d,p)		
	ΔE	ΔH	ΔG	ΔE	ΔH	ΔG
$C_4H_8OS + OH \rightarrow C_3H_7OSC^{\bullet}$ (I1) + H_2O	2.43	−17.92	−19.05	8.47	−16	−17.42
$C_3H_7OSC^{\bullet}$ (I1) + $O_2 \rightarrow C_4H_7OSOO^{\bullet}$ (I2)	No barrier	−28.53	−22.26	No barrier	−35.1	−29.35
$C_4H_7OSOO^{\bullet}$ (I2) + $HO_2 \rightarrow C_4H_7OSOOH^{\bullet} + O_2$ (P1)	1.98	−12.37	−15.1	3.53	−29.95	−32.02
$C_4H_7OSOO^{\bullet}$ (I2) + $NO_2 \rightarrow C_4H_7OSOONO_2^{\bullet}$ (P2)	104.41	73.64	73.87	119.02	52.2	52.88
$C_4H_7OSOO^{\bullet}$ (I2) + $NO \rightarrow C_4H_7OSO^{\bullet}$ (I3) + NO_2	No barrier	−27.94	−27.11	No barrier	−30	−29.37
$C_4H_7OSO^{\bullet}$ (I3) + $NO_2 \rightarrow C_3H_6OS(C=O) + OH + NO^{\bullet}$ (P3)	20.79	14.25	10.6	29.06	22.57	19.76
$C_4H_7OSO^{\bullet}$ (I3) + $NO_2 \rightarrow C_3H_6OS(C=O) + HNO_2$ (P4)	52.81	−31.24	−35.3	66.2	−28.61	−31.7
$C_4H_7OSO^{\bullet}$ (I3) + $O_2 + NO_2 \rightarrow C_3H_6OS(C=O) + O_3 + HNO$ (P5)	67.73	12.75	8.63	79.02	23.61	20.14
$C_4H_7OSO^{\bullet}$ (I3) + $O_2 \rightarrow C_3H_6OS(C=O) + HO_2$ (P6)	8.95	−43.38	−40.56	9.9	−46.14	−44.76
$C_4H_7OSOO^{\bullet}$ (I2) + $C_4H_7OSOO^{\bullet}$ (I2) → $C_4H_7OSO_4C_4H_7OS$ (I4)	No barrier	−24.12	−24.1	No barrier	−37.62	−39.11
$C_4H_7OSO_4C_4H_7OS$ (I4) → $2C_3H_6OS(C=O) + H_2O_2$ (P7)	2.58	−119.71	−124.71	4.64	−124.34	−127.02
$C_4H_7OSO_4C_4H_7OS$ (I4) → $C_3H_6OS(C=O) + C_3H_7OSC(OH) + O_2$ (P8)	25.67	−60.79	−64.04	33.24	−64	−67.55
$C_4H_7OSO_4C_4H_7OS$ (I4) → $C_4H_7OSO_2C_4H_7$ OS $+O_2$ (P9)	31.53	10.41	10.39	35.6	6.12	3.6

Table 2 Energy barrier ΔE (in kcal/mol), enthalpy ΔH (in kcal/mol), and Gibb's free energy ΔG (in kcal/mol) of the favorable reaction pathway corresponding to the reaction of 1,4-thioxane with OH radical calculated at B3LYP and M06-2X functionals using 6-31 + G(d,p) basis set

Reactions	B3LYP			M06-2X		
	ΔE	ΔH	ΔG	ΔE	ΔH	ΔG
$C_4H_8OS + OH \rightarrow C_3H_7OSC^{\bullet}$ (I1) + H_2O	4.1	−19.04	−20.7	8.23	−17.52	−18.21
$C_3H_7OSC^{\bullet}$ (I1) + $O_2 \rightarrow C_4H_7OSOO^{\bullet}$ (I2)	No barrier	−28.27	−20.63	No barrier	−34.54	−28.06
$C_4H_7OSOO^{\bullet}$ (I2) + $HO_2 \rightarrow C_4H_7OSOOH + O_2$ (P1)	3.16	−12.26	−16.98	2.23	−29.28	−31.56

4.6×10^{-13} cm^3 $molecule^{-1}$ s^{-1}. The equilibrium constant for the formation and decomposition of the peroxy radical was found to be 1.25×10^{-17} cm^3 $molecule^{-1}$ at 298 K. This value is fairly comparable with the equilibrium constant for the formation of CH_3SOO peroxy radical [53]. As the adiabatic barrier for the formation of peroxy radical

Table 3 The selected geometrical parameters (bond length, R in Å, bond angle, θ in degrees and dihedral angle, Φ in degrees) on the potential energy surface of the favorable reaction path corresponding to the reaction of 1,4-thioxane with OH radical

Geometrical parameter[a]	B3LYP						M06-2X					
	6-31G(d,p)			6-31+G(d,p)			6-31G(d,p)			6-31+G(d,p)		
	R	TS1	I1	R	TS1	I1	R	TS1	I1	R	TS1	I1
R(C3–O2)	3.6	2.6	3.3	3.7	2.8	3.6	3.1	2.5	3.1	3.7	2.6	3.2
R(C3–H5)	1.1	1.2	2.6	1.1	1.2	2.8	1.1	1.2	2.6	1.1	1.2	2.6
R(H5–O2)	3.4	0.9	0.9	3.5	1.5	0.9	3.2	1.4	0.9	3.4	1.4	0.9
θ(H5–O2–H9)	35	95.2	105.1	35.2	95.1	106.3	47.6	94.4	104	35.8	95.2	106.8
θ(C3–H5–O2)	91.5	160.9	132.1	96.2	160.4	149.6	71.4	150.5	114.6	94.7	153.2	115.5
	I1 + O_2	I2		I1 + O_2	I2		I1 + O_2	I2		I1 + O_2	I2	
R(C3–O2)	3.6	1.4		3.9	1.4		3.8	1.4		3.9	1.4	
R(O2–O3)	1.2	1.3		1.2	1.3		1.2	1.3		1.2	1.3	
θ(C3–O2–O3)	137.5	110.9		117.2	111.4		81.7	110.6		95.4	111.1	
	I1 + HO_2	TS2	P1	I1 + HO_2	TS2	P1	I1 + HO_2	TS2	P1	I1 + HO_2	TS2	P1
R(O3–H8)	2.1	1.5	0.9	2.2	1.5	0.9	2.2	1.7	0.9	2.2	1.6	0.9
R(O4–H8)	0.9	1.1	2.7	0.9	1	3	0.9	1	2.3	0.9	1.1	2.4
θ(O2–O3–H8)	96.5	98.4	100.3	96.7	99.1	100.9	96.3	96.1	101.7	96.1	96.4	102.1
Φ(C3–O2–O3-H8)	121.6	116.6	−72	121.3	116.2	−85.5	119.2	111.3	−76.2	119.2	109.9	−79.9

[a] For labeling of atoms see Figs. 2 and 4

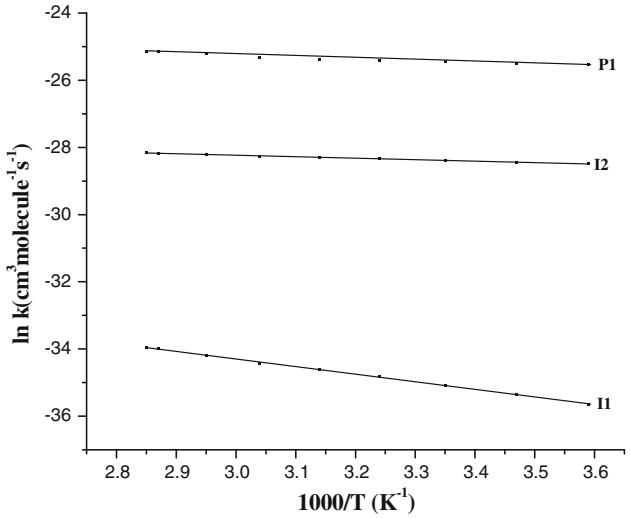

Fig. 10 Arrhenius plot for the rate constants for the formation of thiooxonium radical, I1 peroxy radical, I2 and hydroperoxy-1,4-thioxane, P1

is zero, the tunneling corrections are insignificant for this reaction channel. The calculated Arrhenius activation energy at 298 K is 0.85 kcal/mol. The rate constant k_{P1} calculated at 298 K for the formation of 2-hydroperoxy-1,4-thioxane with O_2 in product channel P1 is 8.8×10^{-12} cm^3 $molecule^{-1}$ s^{-1} and this is comparable with the estimated value based on the reported rate constants for $RO_2 + HO_2$ reactions [54]. The Arrhenius activation energy for this product channel at 298 K is 0.68 kcal/mol. As observed for the initial step, in this H atom abstraction reaction also the tunneling effect is negligible due to the broad energy barrier (imaginary vibrational frequency of TS2 is -559.34 cm^{-1}).

Table 4 Rate constants k_{I1}, k_{I2}, and k_{P1} (in cm^3 $molecule^{-1}$ s^{-1}) for the initial H atom abstraction (I1) step, peroxy radical (I2) formation step and the formation of 2-hydroperoxy-1,4-thioxane + O_2 product channel (P1)

Temperature (K)	$k_{I1} \times 10^{-16}$	$k_{I2} \times 10^{-13}$	$k_{P1} \times 10^{-12}$
278	3.3	4.2	8.1
288	4.4	4.4	8.5
298	5.8	4.6	8.8
308	7.4	4.9	9.2
318	9.3	5.1	9.5
328	11.5	5.3	9.9
338	14.1	5.6	10.2
348	17.1	5.8	10.5
350	17.7	5.9	10.6

Conclusions

The potential energy surface for the atmospheric oxidation of 1,4-thioxane by OH radical has been explored in detail

using quantum chemical methods and the kinetics of the reactions are studied using VTST. From the analysis of the results, the following main conclusions are arrived.

1. The OH radical reaction with 1,4-thioxane proceed mainly by hydrogen atom abstraction from CH_2 group of 1,4-thioxane and this results in the formation of an alkyl radical and the subsequent reaction of this alkyl radical with O_2 yield hydroxyl-1,4-thioxane peroxy radical intermediate in a barrierless reaction.
2. As the secondary reactions, the reaction between hydroxyl-1,4-thioxane peroxy radical and other atmospheric species like HO_2, NO_2, and NO are studied. The reaction between hydroxyl-1,4-thioxane peroxy radical and HO_2 results in the formation of 2-hydroperoxy-1,4-thioxane along with O_2 and this is found to be the most favorable reaction with an activation energy barrier of 3.53 kcal/mol.
3. An alkoxy radical is formed as another important intermediate due to the reaction between hydroxyl-1,4-thioxane peroxy radical and NO. The potential tropospheric degradation of this alkoxy radical is observed due to its reaction with O_2.
4. The hydroxyl-1,4-thioxane peroxy radical undergoes self-reaction in a barrierless fashion to form a linear tetraoxide intermediate complex. This intermediate has sufficient energy to further rearrange to yield atmospheric oxidation products. The dissociation of tetraoxide intermediate into two 1,4-thioxane-2-one carbonyl products along with H_2O_2 is found to be the most favorable self-reaction with a small barrier of 4.64 kcal/mol and with a large exothermicity of −124.34 kcal/mol.
5. The rate constant for the initial H atom abstraction step is found to be 5.8×10^{-16} cm^3 $molecule^{-1}$ s^{-1} at 298 K and the Arrhenius activation energy for this initial reaction is 4.6 kcal/mol.

Acknowledgments One of the authors (K.S.) is thankful to the Department of Science and Technology (DST), India, for granting the research project under DST-Fast track scheme for young scientists. L.S. is thankful to the Department of Science and Technology (DST), India, for awarding INSPIRE Fellowship.

References

1. Atkinson R, Arey J (2003) Chem Rev 103:4605–4638
2. Guenther A, Geron C, Pierce T, Lamb B, Harley P, Fall R (2000) J Atmos Environ 34:2205
3. Guenther A, Hewitt CN, Erickson D, Fall R, Geron C, Graedel T, Harley P, Klinger L, Lerdau M, McKay WA, Pierce T, Scholes B, Steinbrecher R, Tallamraju R, Taylor J, Zimmermann P (1995) J Geophys Res 100:8873
4. Placet M, Mann CO, Gilbert RO, Niefer M (2000) J Atmos Environ 34:2183
5. Sawyer RF, Harley RA, Cadle SH, Norbeck JM, Slott R, Bravo HA (2000) J Atmos Environ 34:2161
6. Wine PH, Thompson RJ (1984) Int J Chem Kinet 16:867
7. Zhang D, Zhang R (2002) J Am Chem Soc 124:2692
8. Seinfeld JH, Pandis SN (1997) Atmospheric chemistry and physics: from air pollution to climate change. Wiley, New York
9. Thomson AM (1988) Science 256:1157
10. Aschmann SM, Atkinson R (2006) J Phys Chem A 110:13029
11. Daykin EP, Wine PH (1990) Int J Chem Kinet 22:1083
12. Martin D, Jourdain JL, Le Bras G (1985) Int J Chem Kinet 17:1247
13. Tuazon EC, Aschmann SM, Atkinson R (2007) J Phys Chem A 111:916
14. Brewer PG, Nakayama N (2008) Environ Sci Technol 42:1394
15. Zhang X, Hester KC, Mancillas O, Peltzer ET, Walz PM, Brewer G (2009) Environ Sci Technol 43:610
16. Aschmann SM, Long WD, Atkinson R (2008) J Phys Chem A 112:13556
17. Lightfoot PD, Cox RA, Crowley JN, Destriau M, Hayman GD, Jenkin ME, Moortgat GK, Zabel F (1992) Atmos Environ 26A:1805
18. Wallington TJ, Dagaut P, Kurylo MJ (1992) Chem Rev 92:667
19. Tyndall GS, Cox RA, Granier C, Lesclaux R, Moortgat GK, Pilling MJ, Ravishankara AR, Wallington TJ (2001) J Geophys Res 106:12157
20. Feria L, Gonzalez C, Castro M (2004) Int J Quant Chem 99:605
21. Feria L, Gonzalez C, Castro M (2004) Int J Quant Chem 96:380
22. Isaacson AD, Truhlar DG, Rai SN, Steckler R, Hancock GC, Garrett BC, Redmon MJ (1987) Comput Phys Commun 47:91
23. Becke AD (1993) J Chem Phys 98:5648
24. Lee C, Yang W, Parr RG (1988) Phys Rev B 37:785
25. Zhao Y, Truhlar DG (2008) Theor Chem Acc 120:215
26. Anglada JM (2004) J Am Chem Soc 126:9809
27. Turecek F (2000) Collect Czech Chem Commun 65:455
28. Zheng J, Zhao Y, Truhlar DG (2007) J Phys Chem A 111:5121
29. Karton A, Tarnopolsky A, Lamere JF, Schatz GC, Martin JML (2008) J Phys Chem A 112:12868
30. Fukui K (1981) Acc Chem Res 14:363
31. Ishida K, Morokuma K, Kormornicki A (1977) J Chem Phys 66:2153
32. Frisch MJ, Trucks GW, Schlegel HB, Scuseria GE, Robb MA, Cheeseman JR, Scalmani G, Barone V, Mennucci B, Petersson GA, Nakatsuji H, Caricato M, Li X, Hratchian HP, Izmaylov AF, Bloino J, Zheng G, Sonnenberg JL, Hada M, Ehara M, Toyota K, Fukuda R, Hasegawa J, Ishida M, Nakajima T, Honda Y, Kitao O, Nakai H, Vreven T, Montgomery JA, Jr., Peralta JE, Bearpark M, Heyd JJ, Brothers E, Kudin KN, Staroverov VN, Kobayashi R, Normand J, Raghavachari K, Rendell A, Burant JC, Iyengar SS, Tomasi J, Cossi M, Rega N, Millam JM, Klene M, Knox JE, Cross JB, Bakken V, Adamo C, Jaramillo J, Gomperts R, Stratmann RE, Yazyev O, Austin AJ, Cammi R, Pomelli C, Ochterski JW, Martin RL, Morokuma K, Zakrzewski VG, Voth GA, Salvador P, Dannenberg JJ, Dapprich S, Daniels AD, Farkas O, Foresman JB, Ortiz JV, Cioslowski J, Fox DJ (2009) Gaussian, Inc, Wallingford, CT
33. Garrett BC, Truhlar DG (1979) J Am Chem Soc 101:4534
34. Garrett BC, Truhlar DG (1979) J Chem Phys 70:1593
35. Garrett BC, Truhlar DG, Grev RS, Magnuson AW (1980) J Phys Chem 84:1730
36. Liu YP, Lynch GC, Truong TN, Lu DH, Truhlar DG, Garrett BC (1993) J Am Chem Soc 115:2408
37. Lu DH, Truong TN, Melissas VS, Lynch GC, Liu YP, Garrett BC, Steckler R, Issacson AD, Rai SN, Hancock GC, Louderdale JG, Joseph T, Truhlar DG (1992) Comput Phys Commun 71:235
38. Chaung YY, Truhlar DG (2000) J Chem Phys 112:1221
39. Truhlar DG (1991) J Comput Chem 12:266

40. Zheng J, Zhang S, Corchado JC, Chuang YY, Coitino EL, Ellingson BA, Truhlar DG (2009) GAUSSRATE version
41. Zheng J, Zhang S, Lynch BJ, Corchado JC, Chaung YY, Fast PL, Hu WP, Liu YP, Lynch GC, Nguyen KA, Jackels CF, Ramos AF, Ellingson BA, Melissas VS, Villa J, Rossi I, Coitino EL, Pu J, Albu TV (2010) POLYRATE version
42. Raoult S, Rayez MT, Rayez JC, Lesclaux R (2004) Phys Chem Chem Phys 6:2245
43. Barnes I, Hjorth J, Mihalopoulos N (2006) Chem Rev 106:940
44. Li Z, Nguyen P, Leon MF, Wang JH, Han K, He GZ (2006) J Phys Chem A 110:2698
45. Williams MB, Jost PC, Cossairt BM, Hynes AJ (2007) J Phys Chem A 111:89
46. Barone SB, Turnipshed AA, Ravishankara AR (1996) J Phys Chem 100:14694
47. Zavala CO, Galano A (2009) J Chem Theory Comput 5:1295
48. Silva G, Hamdan MR, Bozzalli JW (2009) J Chem Theory Comput 5:3185
49. Hou H, Deng L, Li J, Wang B (2005) J Phys Chem A 109:9299
50. Finlayson-Pitts BJ, Pitts JN Jr (1997) Science 276:1045
51. Aschmann SM, Long WD, Atkinson R (2006) J Phys Chem A 110:7393
52. IUPAC. http://www.iupac-kinetic.ch.cam.ac.uk (2004) 1
53. Koch LC, Marshall P, Ravishankara AR (2004) J Phys Chem A 108:5205
54. Butkovskaya NI, Bras LG (1994) J Phys Chem 98:2582